

# A Quantum Chemical Study of $\text{Cu}^{2+}$ Interacting with Guanine–Cytosine Base Pair. Electrostatic and Oxidative Effects on Intermolecular Proton-Transfer Processes

Marc Noguera, Joan Bertran,\* and Mariona Sodupe\*

Departament de Química, Universitat Autònoma de Barcelona, Bellaterra 08193

Received: August 29, 2003; In Final Form: October 24, 2003

The influence of metal cations ( $\text{M} = \text{Cu}^+$ ,  $\text{Ca}^{2+}$  and  $\text{Cu}^{2+}$ ) coordinated to  $\text{N}_7$  of guanine on the intermolecular proton-transfer reaction in guanine–cytosine base pair has been analyzed using the B3LYP density functional approach. Gas phase metal cation interaction stabilizes the ion pair structure derived from the  $\text{N}_1$ – $\text{N}_3$  single-proton-transfer reaction, the effects being more pronounced for the divalent cations than for the monovalent one. For  $\text{Cu}^{2+}\text{GC}$  the reaction is largely favored due to both electrostatic and oxidative effects. Hydration of the metal cation disfavors the reaction due to the screening of electrostatic effects. However, for  $\text{Cu}^{2+}$  the reaction can still be easily produced, especially for certain local environments of the metal cation for which  $\text{Cu}^{2+}$  induces the oxidation of guanine. Therefore, the ability of  $\text{Cu}^{2+}$  to oxidize guanine turns out to be a key factor for this mutagenic process.

## I. Introduction

Metal cations are known to play an important role in both the stabilization and destabilization of DNA.<sup>1,2</sup> The main effect of metal cations is to neutralize the negatively charged backbone phosphate groups through nonspecific electrostatic interactions, which stabilizes the double helix. In particular, alkali-metal ions can lead to partial charge neutralization by condensing around DNA in a cylindrical fashion. In addition, metal cations can specifically coordinate to the phosphate oxygen atoms, sugar oxygen atoms or electron donor groups of the heterocyclic bases, the different coordinations depending on the concentration and on the kind of metal cation. For instance, alkali-metal and alkaline-earth-metal cations interact mostly with the phosphate group, whereas transition-metal cations such as  $\text{Zn}^{2+}$  and  $\text{Cu}^{2+}$  frequently bind directly (inner-shell coordination) to the nucleobase. Therefore, although cation–phosphate interactions are predominant, the binding of metal ions to the bases is not negligible, especially at high concentrations, which can modify the hydrogen bonding and the stacking interactions that stabilize the double helix.

It is well-known that the  $\text{N}_7$  position of guanine, which is readily accessible in the major groove of duplex DNA, and is not involved in Watson–Crick base pairing, is the preferred metal binding site.<sup>1–4</sup> Moreover, the large dipole moment of guanine ( $>7$  D) and its orientation favor this major metal binding pattern. Many studies have analyzed the interaction of different metal cations to guanine<sup>4–10</sup> and their influence on base pairing.<sup>7–14</sup> Results show that metal cation binding to base pairs has a pronounced effect on structural and electronic properties of the interacting bases, the stability of guanine–cytosine Watson–Crick base pairing being enhanced<sup>7–13</sup> mainly by polarization.<sup>9,12</sup> Moreover, a few theoretical results have shown that the presence of metal cations interacting at the  $\text{N}_7$  position of guanine promotes the proton transfer from  $\text{N}_1$  of guanine to the  $\text{N}_3$  acceptor site of cytosine.<sup>9,10</sup> However, the screening of the metal charge by the environment (water

molecules and phosphate) reduces significantly the probability of such a mutagenic process.<sup>15</sup>

Most of the theoretical studies performed on the interaction of metal cations with guanine or guanine–cytosine base pair have dealt with alkali, alkaline-earth, or closed-shell transition-metal cations. Only one study<sup>16</sup> has analyzed the interaction of  $\text{Cu}^{2+}$ , a  $d^9$  open-shell cation, with guanine, but its influence on base pairing or intermolecular proton-transfer processes was not considered.  $\text{Cu}^{2+}$  is an important biological metal ion with a rich redox chemistry and closely associated with DNA bases,<sup>17</sup> particularly guanine. In the presence of  $\text{H}_2\text{O}_2$ , and often with added ascorbic acid, copper ion has been shown to induce DNA base damage.<sup>18–22</sup> It has been suggested that such damage is induced through the formation of a  $\text{DNA}-\text{Cu}^+-\text{H}_2\text{O}_2$  complex, which results in oxidation of  $\text{Cu}^+$  to lead  $\text{Cu}^{2+}$ –DNA and base modification. Thus, the structural and electronic effects induced by the interaction of  $\text{Cu}^{2+}$  on guanine–cytosine base pairing are of great interest. Moreover, due to the oxidant character of  $\text{Cu}^{2+}$ , its interaction with guanine–cytosine base pair might lead to the formation of oxidized guanine, which has been previously shown to favor the proton transfer from  $\text{N}_1$  to the  $\text{N}_3$  of cytosine.<sup>23</sup>

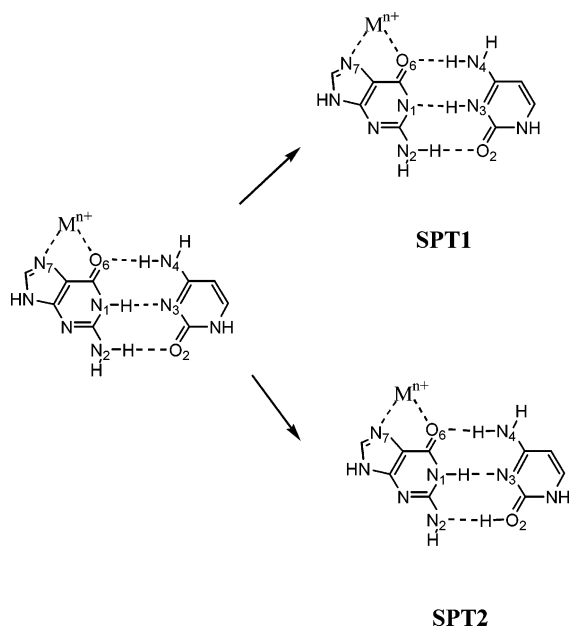
The main goal of this paper is to theoretically analyze the effect of coordination of  $\text{Cu}^{2+}$ , an open-shell ( $d^9$ ) metal cation in which both electrostatic and oxidative effects are important, on guanine–cytosine (GC) Watson–Crick base pairing and on different intermolecular proton-transfer reactions. Results will be compared with those obtained for  $\text{Cu}^+$  and  $\text{Ca}^{2+}$  for which the metal–GC interaction is mainly due to electrostatic and polarization effects. First, we will present the results obtained in the gas phase. Finally, the changes produced in both the electrostatic and oxidant effects upon coordinating the metal cation to different water molecules will be discussed.

## II. Methods

Molecular geometries and harmonic vibrational frequencies of the considered structures have been obtained using the nonlocal hybrid three-parameter B3LYP density functional

\* Corresponding authors. E-mail: J.B., bertran@klingon.uab.es; M.S., mariona@klingon.uab.es.

## SCHEME 1



approach,<sup>24</sup> as implemented in the Gaussian 98<sup>25</sup> set of programs package. Previous theoretical calculations have shown that the B3LYP approach is a cost-effective method for studying transition-metal ligand systems.<sup>26</sup>

Geometry optimizations and frequency calculations have been performed using the following basis sets. The Cu basis set is based on the (14s9p5d) primitive set of Wachters<sup>27</sup> supplemented with one s, two p, and one d diffuse functions<sup>28</sup> as well as one f polarization function,<sup>29</sup> the final contracted basis set being [10s7p4d1f]. The Ca basis set is the (14s11p3d)/[8s7p1d] of Blaudeau et al.<sup>30</sup> supplemented with one s, p, and d diffuse functions. Thus, the final contracted basis set is [9s8p2d]. For C, N, O, and H we have used the 6-31G(d,p) basis set. This basis set will be denoted hereafter as B1. Energy calculations have also been carried out using the larger 6-31++G(d,p) basis set for C, N, O, and H. This basis set will be referred to as B2. For the smaller basis set, the base pairing energies have been corrected for basis set superposition error using the counterpoise method.<sup>31</sup>

Thermodynamic corrections have been obtained by assuming an ideal gas, unscaled harmonic vibrational frequencies, and the rigid rotor approximation by standard statistical methods.<sup>32</sup> Net atomic charges and spin densities have been obtained using the natural population analysis of Weinhold et al.<sup>33</sup> Open-shell calculations have been performed using an unrestricted formalism. All calculations have been performed with Gaussian 98 package.<sup>25</sup>

### III. Results and Discussion

As mentioned the N<sub>7</sub> position of guanine is the preferred metal binding site.<sup>1-4</sup> Because of that, we have only considered the interaction of the metal cation at this position. Scheme 1 shows the two single-proton-transfer processes studied in the present work: the N<sub>1</sub>-N<sub>3</sub> (SPT1) and the N<sub>2</sub>-O<sub>2</sub> one (SPT2). Although the SPT1 transfer is the most favorable one, the SPT2 has also been found to be possible for Cu<sup>2+</sup>.

As expected, the products resulting from a double proton-transfer reaction (N<sub>1</sub>-N<sub>3</sub> and N<sub>4</sub>-O<sub>6</sub>) were not found to be stable and any attempt to localize them collapsed to the single-proton-transfer minima.

**TABLE 1: B3LYP/B1 Metal-Ligand and Hydrogen Bond Distances (Å) for the Non-Proton-Transferred GC and Single-Proton-Transferred SPT1 and SPT2 Structures**

	GC	[GC] <sup>+</sup>		
		GC	TS-SPT1	SPT1
O <sub>6</sub> -N <sub>4</sub>	2.79	2.97	2.73	2.70
N <sub>1</sub> -N <sub>3</sub>	2.93	2.82	2.63	2.80
N <sub>2</sub> -O <sub>2</sub>	2.92	2.67	2.71	2.93
Ca <sup>2+</sup>				
	GC	TS-SPT1	SPT1	
Ca <sup>2+</sup> -N <sub>7</sub>	2.32	2.30	2.29	
Ca <sup>2+</sup> -O <sub>6</sub>	2.17	2.16	2.15	
O <sub>6</sub> -N <sub>4</sub>	3.20	2.90	2.95	
N <sub>1</sub> -N <sub>3</sub>	2.87	2.65	2.92	
N <sub>2</sub> -O <sub>2</sub>	2.66	2.68	2.92	
Cu <sup>+</sup>				
	GC	TS-SPT1	SPT1	
Cu <sup>+</sup> -N <sub>7</sub>	2.01	2.00	2.00	
Cu <sup>+</sup> -O <sub>6</sub>	2.12	2.08	2.07	
O <sub>6</sub> -N <sub>4</sub>	3.00	2.72	2.70	
N <sub>1</sub> -N <sub>3</sub>	2.86	2.64	2.79	
N <sub>2</sub> -O <sub>2</sub>	2.77	2.80	2.95	
Cu <sup>2+</sup>				
	GC	TS-SPT1	SPT1	SPT2
Cu <sup>2+</sup> -N <sub>7</sub>	2.04	2.05	2.06	2.03
Cu <sup>2+</sup> -O <sub>6</sub>	2.24	2.21	2.14	2.23
O <sub>6</sub> -N <sub>4</sub>	3.16	3.01	3.04	3.25
N <sub>1</sub> -N <sub>3</sub>	2.76	2.66	2.92	2.92
N <sub>2</sub> -O <sub>2</sub>	2.51	2.55	2.85	2.65

**A. Naked Metals (M = Ca<sup>2+</sup>, Cu<sup>+</sup>, and Cu<sup>2+</sup>).** The optimized metal-guanine and H-bond distances of the non-transferred, GC, single-proton-transferred, SPT1 and SPT2, and the corresponding transition states are given in Table 1. For comparison we have also included the values corresponding to isolated neutral and oxidized GC.<sup>23a</sup> For the neutral system the single-proton-transfer structure is not stable because the process implies the formation of an ion pair.

First of all, it must be mentioned that all M<sup>n+</sup>-GC systems have C<sub>s</sub> symmetry, the lowest electronic state being a <sup>1</sup>A' for Ca<sup>2+</sup> and Cu<sup>+</sup> and a <sup>2</sup>A'' for Cu<sup>2+</sup>. In all cases, the metal cation interacts with both the N<sub>7</sub> and O<sub>6</sub> of guanine; that is, the complex shows a bidentate coordination. However, the metal-ligand distances indicate that Ca<sup>2+</sup> cation has a larger affinity for O<sub>6</sub>, whereas Cu<sup>+</sup> and Cu<sup>2+</sup> show a larger preference for N<sub>7</sub>. The largest metal-ligand distances correspond to Ca<sup>2+</sup>. This was to be expected considering that, among the three cations, Ca<sup>2+</sup> is the one with a larger ionic radius. However, in contrast to what one would have initially expected, the metal-ligand distances for Cu<sup>2+</sup> are larger than for Cu<sup>+</sup>. This is due to the fact that the interaction of Cu<sup>2+</sup> induces an oxidation of the base pair so that the final situation can be viewed as the interaction of Cu<sup>+</sup> (d<sup>10</sup>) with the GC<sup>•+</sup> radical cation, which produces an increase of the metal-guanine distances due to the repulsive electrostatic term between the two fragments. Accordingly, the open-shell orbital of [CuGC]<sup>2+</sup>, shown in Figure 1, is mainly centered on the guanine monomer. Moreover, net charges and spin densities of the three different fragments (M<sup>n+</sup>, G, and C), obtained from natural population analysis (Table 2), confirm that Cu<sup>2+</sup> induces an oxidation of guanine. It can be observed that the spin density on [CuGC]<sup>2+</sup> mainly lies on guanine and not on the metal ion, as one would expect for a d<sup>9</sup> metal cation. Moreover, the charge of the metal cation

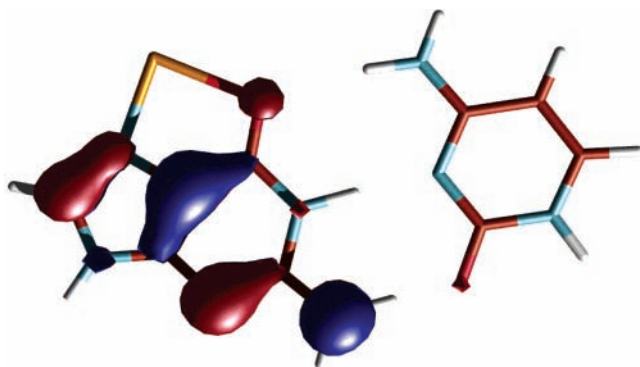
Figure 1. Open-shell orbital of Cu<sup>2+</sup>GC.

TABLE 2: Charges (Spin Densities) from Natural Population Analysis

	GC	[GC] <sup>+</sup>	Ca <sup>2+</sup> –GC	Cu <sup>+</sup> –GC	Cu <sup>2+</sup> –GC
M <sup>n+</sup>			1.85	0.85	0.90(0.00)
G	−0.03	0.85(1.00)	−0.01	0.04	0.81(0.98)
C	0.03	0.15(0.00)	0.16	0.11	0.29(0.02)
SPT1					
M <sup>n+</sup>			1.83	0.83	0.88(0.00)
G <sub>(−H<sup>+</sup>)</sub>		0.08(1.00)	−0.75	−0.67	0.16(1.00)
C <sub>(+H<sup>+</sup>)</sub>		0.92(0.00)	0.92	0.84	0.96(0.00)
SPT2					
M <sup>n+</sup>					0.89(0.00)
G <sub>(−H<sup>+</sup>)</sub>					0.18(1.00)
C <sub>(+H<sup>+</sup>)</sub>					0.93(0.00)

is close to 1 and similar to that obtained for Cu<sup>+</sup>–GC whereas the charge and spin distribution of the base pair is very similar to that of ionized GC<sup>+</sup>.<sup>23a</sup>

With respect to the H-bond distances it can be observed in Table 1 that the binding of the metal cation induces important changes. For all M<sup>n+</sup>–GC systems, the O<sub>6</sub>–N<sub>4</sub> hydrogen bond increases whereas the other two, N<sub>1</sub>–N<sub>3</sub> and N<sub>2</sub>–O<sub>2</sub>, decrease, especially the latter one. Such changes follow the same trend observed for ionized GC<sup>+</sup>. The metal cation interaction strengthens those hydrogen bonds in which guanine acts as proton donor and weakens the one in which it acts as proton acceptor. Similar trends have been observed in previous theoretical studies.<sup>11</sup> As expected, the changes on the hydrogen bond distances are more pronounced for the divalent cations than for the monovalent ones. However, the comparison between the two divalent cations, Ca<sup>2+</sup> and Cu<sup>2+</sup>, shows that the strengthening of the N<sub>1</sub>–N<sub>3</sub> and N<sub>2</sub>–O<sub>2</sub> bonds is significantly larger for Cu<sup>2+</sup>. As mentioned, this is due to the oxidant character of Cu<sup>2+</sup>, which leads to the formation of the Cu<sup>+</sup>–GC<sup>+</sup> complex, for which both the electrostatic and oxidant effects contribute to the changes observed. The comparison between GC<sup>+</sup> and Cu<sup>+</sup>–GC shows that the effect of oxidation is more important than that produced by the binding of a monovalent metal cation.

Several factors contribute to modify the strength of hydrogen bonds when the metal cation interacts at the N<sub>7</sub> position of guanine. On one hand, the presence of the metal cation leads to a repulsive electrostatic interaction between the positive charge of the metal and that of the hydrogens involved in the H-bonds, which strengthens the N<sub>1</sub>–N<sub>3</sub> and N<sub>2</sub>–O<sub>2</sub> bonds and weakens the O<sub>6</sub>–N<sub>4</sub> one. On the other hand, the binding of the metal cation modifies the electron density (mainly that of guanine) due to polarization effects. Finally, the charge transfer from guanine to the metal cation, which is especially important in the case of Cu<sup>2+</sup>, also contributes to the observed changes.

TABLE 3: Net Atomic Charges and  $\sigma$  and  $\pi$  Electron Population at O<sub>6</sub>, N<sub>1</sub>, and N<sub>2</sub> of Guanine<sup>a</sup>

	net atomic charge	$\sigma$	$\pi$
GC			
O <sub>6</sub>	−0.68	7.11	1.57
N <sub>1</sub>	−0.65	6.03	1.62
N <sub>2</sub>	−0.84	6.10	1.74
GC <sup>+</sup>			
O <sub>6</sub>	−0.54(+0.14)	7.12(+0.01)	1.42(−0.15)
N <sub>1</sub>	−0.65(0.00)	6.06(+0.03)	1.59(−0.03)
N <sub>2</sub>	−0.72(+0.12)	6.19(+0.09)	1.53(−0.21)
Ca <sup>2+</sup> –GC			
O <sub>6</sub>	−0.88(−0.20)	7.15(+0.04)	1.73(+0.16)
N <sub>1</sub>	−0.60(+0.05)	6.05(+0.02)	1.55(−0.07)
N <sub>2</sub>	−0.76(+0.08)	6.16(+0.06)	1.60(−0.14)
Cu <sup>+</sup> –GC			
O <sub>6</sub>	−0.76(−0.08)	7.11(0.00)	1.65(+0.08)
N <sub>1</sub>	−0.62(+0.03)	6.04(+0.01)	1.58(−0.04)
N <sub>2</sub>	−0.79(+0.05)	6.14(+0.04)	1.65(−0.09)
Cu <sup>2+</sup> –GC			
O <sub>6</sub>	−0.68(0.00)	7.12(+0.01)	1.56(−0.01)
N <sub>1</sub>	−0.63(+0.02)	6.07(+0.04)	1.56(−0.06)
N <sub>2</sub>	−0.63(+0.21)	6.26(+0.16)	1.37(−0.37)

<sup>a</sup> In parentheses are variations with respect to the values in neutral guanine–cytosine.

To analyze the changes produced on the electron density of guanine upon metal cationization and their influence on the H-bonds, we present in Table 3 the net atomic charges and electron population of O<sub>6</sub>, N<sub>1</sub>, and N<sub>2</sub> of guanine in GC, GC<sup>+</sup>, and M<sup>n+</sup>–GC. According to the symmetry of the system (*C<sub>s</sub>*) the electron population has been decomposed in two components: the  $\sigma$  (*a'*) and  $\pi$  (*a''*) ones. Relative values with respect to isolated neutral GC are included in parentheses. First of all, it can be observed that the  $\pi$  variations are significantly more important than the  $\sigma$  ones. This is not surprising considering that the  $\pi$  system is more polarizable. For Cu<sup>+</sup> and Ca<sup>2+</sup>, metal binding leads to an increase of the electron population at O<sub>6</sub> and so, the net atomic charge becomes more negative. In contrast, a decrease is observed at the N<sub>1</sub> and N<sub>2</sub> atoms, the net atomic charges becoming less negative. As expected, variations are more important for the divalent system. As a consequence of these changes the N<sub>1</sub>–H<sup>34</sup> and N<sub>2</sub>–H become more acidic. The O<sub>6</sub> site does not become more basic, despite the increase of charge density, due to the presence of the metal cation. The Cu<sup>2+</sup>–GC system shows a somewhat different behavior; that is, the charge density at O<sub>6</sub> does not increase, in contrast to what is observed for Ca<sup>2+</sup>, and there is a very important decrease at N<sub>2</sub>. Again, this is due to the oxidant character of Cu<sup>2+</sup>, the resulting changes being a combination of those observed for GC<sup>+</sup> and Cu<sup>+</sup>–GC.

Both the electrostatic repulsion between the metal cation and the hydrogens involved in the H-bonds and the electronic polarization induced by the metal interaction contribute to strengthen the N<sub>1</sub>–N<sub>3</sub> and N<sub>2</sub>–O<sub>2</sub> bonds. However, the O<sub>6</sub>–N<sub>4</sub> bond is weakened, despite the increase on the charge density at O<sub>6</sub>. Thus, the electrostatic repulsive interaction seems to be dominant in this case.

The changes on the hydrogen bonds when metal cations interact with guanine result in an enhancement of the base pairing. The guanine–cytosine interaction energies for isolated G–C and M<sup>n+</sup>G–C (M = Ca<sup>2+</sup>, Cu<sup>+</sup>, and Cu<sup>2+</sup>) are given in Table 4. Counterpoise-corrected values with the smaller basis set B1 are included in parentheses whereas italic numbers correspond to those with the larger B2 basis set. It is observed that the counterpoise correction decreases the guanine–cytosine

**TABLE 4: Interaction Energies Computed at the B3LYP Level with Basis Sets B1 and B2 (kcal/mol)<sup>a</sup>**

	M <sup>n+</sup> G–C			
	G–C <sup>b</sup>	Ca <sup>2+</sup> G–C	Cu <sup>+</sup> G–C	Cu <sup>2+</sup> G–C
<i>D<sub>e</sub></i> <sup>c</sup>	30.3(25.5) 26.2	45.8(42.1) 40.9	38.7(35.5) 34.0	66.4(63.3) 60.4
<i>D<sub>0</sub></i>	28.8(24.0)	44.8(41.1)	36.9(33.7)	67.2(64.1)
$\Delta H_{298K}^0$	28.8(24.0)	44.8(41.1)	37.1(33.9)	67.3(64.2)
$\Delta G_{298K}^0$	17.4(12.6)	33.4(29.7)	24.3(21.1)	54.4(51.3)
	M <sup>n+</sup> –GC			
	Ca <sup>2+</sup> –GC	Cu <sup>+</sup> –GC	Cu <sup>2+</sup> –GC	
<i>D<sub>e</sub></i> <sup>d</sup>	177.3(172.4) 167.5	104.0(98.4) 95.0	343.9(340.3) 330.3	
<i>D<sub>0</sub></i>	176.2(171.3)	102.6(97.0)	345.2(341.6)	
$\Delta H_{298K}^0$	176.8(171.9)	103.1(97.5)	345.8(342.2)	
$\Delta G_{298K}^0$	169.7(164.8)	97.7(92.1)	336.3(332.7)	

<sup>a</sup> In parentheses are counterpoise-corrected values. <sup>b</sup> Taken from ref 23a. <sup>c</sup>  $D_e = E(M^{n+}G) + E(C) - E(M^{n+}GC)$ . <sup>d</sup>  $D_e = E(M^{n+}) + E(GC) - E(M^{n+}GC)$ .

dimerization energies by about 3–5 kcal/mol, the corrected values being in quite good agreement with those obtained with the larger B2 basis set. For all systems, metal cation interaction increases the base pair dissociation energy. With the B2 basis set this increase is 14.7 kcal/mol for Ca<sup>2+</sup>, 7.8 kcal/mol for Cu<sup>+</sup>, and 34.2 kcal/mol for Cu<sup>2+</sup>. Although a larger increase was to be expected for the divalent cations, it is remarkable the important base pairing enhancement produced by Cu<sup>2+</sup> compared to Ca<sup>2+</sup>. Again this is due to the fact that Cu<sup>2+</sup> oxidizes the base pair and, so, part of this important increase results from the formation of GC<sup>•+</sup> radical cation. Note that the observed increase of 34.2 kcal/mol is about 9 kcal/mol larger than the value that one would obtain considering that both ionization (17.6 kcal/mol) and Cu<sup>+</sup> cationization (7.8 kcal/mol) effects are additive, which points out important cooperative effects. A similar base pairing energy has been obtained for Na<sup>+</sup>G<sup>•+</sup>C (55.4 kcal/mol), which confirms that the metal cation oxidizes guanine to lead to Cu<sup>+</sup>G<sup>•+</sup>C. The results obtained for Ca<sup>2+</sup> and Cu<sup>+</sup> are similar to those reported in previous theoretical studies.<sup>11a</sup>

Metal–GC interaction energies have also been included in Table 4. As expected, metal–GC interaction energies are larger for the divalent cations (Ca<sup>2+</sup> and Cu<sup>2+</sup>) than for the monovalent one (Cu<sup>+</sup>). Large differences observed between Ca<sup>2+</sup> and Cu<sup>2+</sup> mainly arise from the oxidant character of Cu<sup>2+</sup>. Note that the difference between the Cu<sup>2+</sup>+GC and Cu<sup>+</sup>+GC<sup>•+</sup> asymptotes is 322.1 kcal/mol with the large basis set. Moreover, the interaction between Cu<sup>+</sup> and GC<sup>•+</sup> is stabilizing by 8.2 kcal/mol due to polarization of the base pair.

It has been observed that metal binding of GC strengthens those H-bonds in which guanine acts as proton donor (N<sub>1</sub>–N<sub>3</sub> and N<sub>2</sub>–O<sub>2</sub>) and weakens the one in which it acts as proton acceptor (O<sub>6</sub>–N<sub>4</sub>). Thus, any of the two strengthened H-bonds can be involved in the single-proton-transfer reaction (see Scheme 1). Results show that the transfer from N<sub>1</sub> to N<sub>3</sub> (SPT1) is the only possible process for Ca<sup>2+</sup> and for Cu<sup>+</sup>, because all attempts to optimize the proton-transferred structure resulting from the N<sub>2</sub>–O<sub>2</sub> transfer (SPT2) collapsed to the initial one. However, for Cu<sup>2+</sup> both the SPT1 and SPT2 structures were obtained. The fact that the SPT2 structure is only obtained for Cu<sup>2+</sup> is consistent with the fact that its interaction to GC leads to a very strong N<sub>2</sub>–O<sub>2</sub> hydrogen bond due to its oxidant character. It should be mentioned that the SPT2 complex has also been found for Na<sup>+</sup>G<sup>•+</sup>C, which shows that both electro-

static and oxidant effects are important to stabilize this structure. However, the SPT2 structure is less stable than the SPT1 one due to the rigidity of the bases, which do not benefit alternate situations with a different central H-bond. Moreover, the proton affinity at the O<sub>2</sub> site of cytosine is smaller than that of N<sub>3</sub>.<sup>35</sup>

The metal–ligand and hydrogen bond distances of SPT1 and SPT2 are shown in Table 1, and the charges and spin densities in Table 2. In general, metal–guanine distances slightly decrease in the proton-transferred SPT1 and SPT2 structures. For Ca<sup>2+</sup> and Cu<sup>+</sup> this is consistent with the fact that the guanine fragment G<sup>–(H<sup>+</sup>)</sup> acquires a certain negative charge (see Table 2), which enhances the metal–guanine binding. For Cu<sup>2+</sup>, the decrease of the M–O<sub>6</sub> distance is attributed to the fact that the positive charge of ionized guanine mainly moves to protonated cytosine, diminishing its electrostatic repulsion with Cu<sup>+</sup>.

Hydrogen bond distances experience significant changes. For the SPT1 structure with Cu<sup>+</sup>, it is observed that those hydrogen bonds in which protonated cytosine, C<sup>+(H<sup>+</sup>)</sup> acts as a proton donor (O<sub>6</sub>–N<sub>4</sub> and N<sub>1</sub>–N<sub>3</sub>) become shorter whereas the one in which it acts as a proton acceptor (N<sub>2</sub>–O<sub>2</sub>) becomes longer compared to the nontransferred system. This was to be expected considering that cytosine supports a positive charge, which makes N<sub>3</sub>–H and N<sub>4</sub>–H bonds more acidic and the O<sub>2</sub> a poorer proton acceptor. Moreover, because guanine acquires an important negative charge the O<sub>6</sub> and N<sub>1</sub> centers involved in the H-bonds become more basic. Globally, the proton-transferred structure shows shorter H-bonds than the nontransferred one, indicating a stronger interaction between the two fragments, G<sup>–(H<sup>+</sup>)</sup> and C<sup>+(H<sup>+</sup>)</sup>.

Ca<sup>2+</sup> and Cu<sup>2+</sup> present a somewhat different behavior. For Ca<sup>2+</sup>G<sup>–(H<sup>+</sup>)</sup>–C<sup>+(H<sup>+</sup>)</sup> the repulsive electrostatic interaction between the divalent metal cation and protonated cytosine, C<sup>+(H<sup>+</sup>)</sup>, becomes dominant, which does not allow O<sub>6</sub>–N<sub>4</sub> and N<sub>1</sub>–N<sub>3</sub> bonds to become as strong as for Cu<sup>+</sup>. For Cu<sup>2+</sup> we get a Cu<sup>+</sup>G<sup>•(H<sup>+</sup>)</sup>–C<sup>+(H<sup>+</sup>)</sup> complex; the G<sup>•(H<sup>+</sup>)</sup> fragment does not acquire a negative charge (see Table 2) and again the repulsive interaction between the metal cation and the positive C<sup>+(H<sup>+</sup>)</sup> becomes dominant. Therefore, for Ca<sup>2+</sup> and Cu<sup>2+</sup> one observes a clear weakening of the hydrogen bonds.

The relative energies of the single-proton-transferred structure with respect to the M<sup>n+</sup>G+C asymptote are given in Figure 2. For comparison we have also included the relative energies of the single-proton-transfer M<sup>n+</sup>G<sup>–(H<sup>+</sup>)</sup>+C<sup>+(H<sup>+</sup>)</sup> asymptote. Although relative energies with the larger basis set are 4–6 kcal/mol smaller in absolute value due to smaller basis set superposition error, the energy barriers and reaction energies with the two basis sets are very similar. As expected, metal cation interaction stabilizes the ion pair complex. Note that in the absence of a metal cation the G<sup>–(H<sup>+</sup>)</sup>–C<sup>+(H<sup>+</sup>)</sup> structure is estimated to lie about 19 kcal/mol above GC.<sup>36</sup> For the monovalent Cu<sup>+</sup>, the reaction energy (5.1 kcal/mol with B2) decreases significantly, the energy barrier being 6.9 kcal/mol. For the divalent Ca<sup>2+</sup> and Cu<sup>2+</sup>, the electrostatic effects are larger and the proton-transfer reaction leading to the SPT1 species becomes even more favorable (–3.8 and –10.1 kcal/mol, respectively), and consequently present smaller energy barriers (3.2 and 0.5 kcal/mol). For Cu<sup>2+</sup>, the proton-transfer reaction leading to the SPT2 structure (–2.1 kcal/mol) is less favorable than the one that leads to SPT1 (–10.1 kcal/mol).

The most important difference between the monovalent Cu<sup>+</sup> and the divalent Ca<sup>2+</sup> and Cu<sup>2+</sup> cations is that for Cu<sup>+</sup> the proton-transferred M<sup>n+</sup>G<sup>–(H<sup>+</sup>)</sup>+C<sup>+(H<sup>+</sup>)</sup> asymptote lies 15.5 kcal/mol above the ground-state M<sup>n+</sup>G+C one, and so, the M<sup>n+</sup>G<sup>–(H<sup>+</sup>)</sup>–C<sup>+(H<sup>+</sup>)</sup> H-bond interaction (44.4 kcal/mol) is

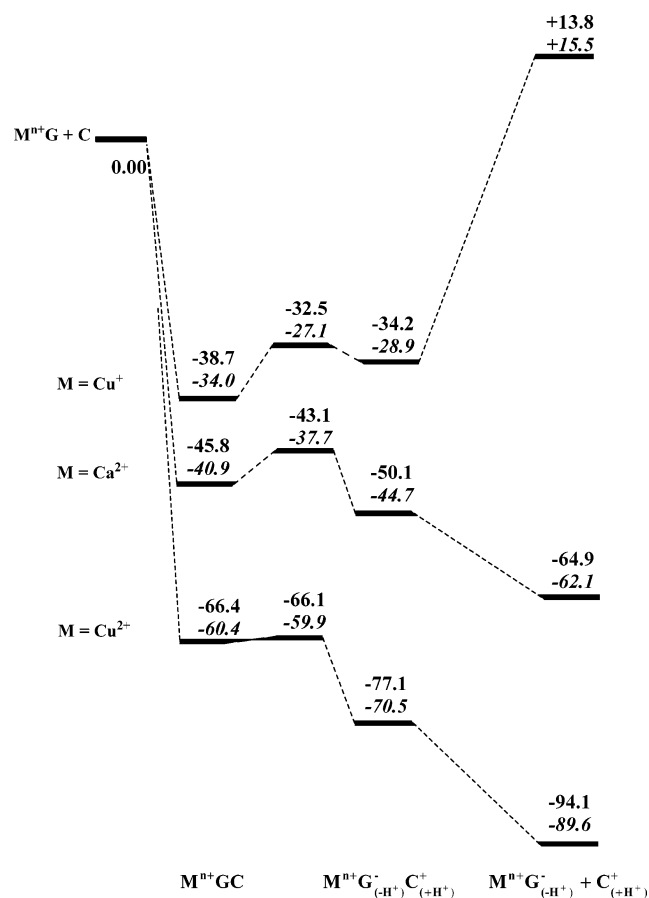


**Figure 2.** Energy profiles corresponding to the single-proton-transfer SPT1 reaction in  $M^{n+}GC$  ( $M = Ca^{2+}$ ,  $Cu^+$ , and  $Cu^{2+}$ ) systems. Relative energies (in kcal/mol) with basis sets B1 and B2.

significantly larger than in  $MG-C$  (34.0 kcal/mol). Consistently, the hydrogen bond distances in the proton-transferred structure are shorter than in the initial species (see above). In contrast, for the divalent cations the proton-transferred asymptote lies significantly below the  $M^{n+}G^-(_{-H^+})-C^+(_{+H^+})$  SPT1 structure. Because of that and considering the small energy barrier of the single-proton-transferred reaction, the interaction of these metal cations to guanine is expected to induce a spontaneous proton-transfer process followed by the separation of the two fragments. This is due to the important electrostatic repulsion between the two,  $M^{n+}G^-(_{-H^+})$  and  $C^+(_{+H^+})$ , positively charged systems. Finally, it should be mentioned that although both divalent cations show a similar behavior, the oxidant character of  $Cu^{2+}$  along with the electrostatic effects make the single-proton-transfer process more efficient.

**B. Hydrated Metal Cations.** The results presented in the previous section correspond to the gas phase situation, which can be very different from the one in real living systems, given that in these cases the metal cation is solvated by water molecules and interacting with the negatively charged backbone. Therefore, the electrostatic effects will be largely screened, which will make less favorable the proton-transfer reaction. In fact, previous<sup>9</sup> single-point calculations have shown that both minima are isoenergetic for pentahydrated  $Mg^{2+}$  and that the reaction becomes unfavorable by about 13 kcal/mol if one water molecule is replaced by an  $OH^-$  so that the total charge is +1. Although the changes induced by cation solvation on the electrostatic interactions are to be expected, the changes on the oxidant character as well as the contribution of the two effects can be more complex. Moreover, whereas  $Mg^{2+}$  is commonly

hexacoordinated with a fairly rigid coordination sphere,<sup>37</sup> transition-metal cations such as  $Cu^+$ <sup>38,39</sup> or  $Zn^{2+}$ <sup>40</sup> can have a more flexible coordination sphere. Thus, the screening of electrostatic effects and more importantly the changes in the oxidant character of  $Cu^{2+}$  may change significantly with the number of water molecules directly coordinated to the metal cation.

In this section we will mainly focus on the effect of water solvation on  $Ca^{2+}$  and  $Cu^{2+}$ , because for these two metal cations the gas phase results have shown that the single-proton-transfer reaction occurs very easily, especially in the case of  $Cu^{2+}$ . For  $Cu^+$ , the gas phase reaction energy has been found to be positive and electrostatic screening due to water solvation would disfavor the reaction even more. Hydrated cations have been found to form inner sphere contacts with either  $O_6$  or  $N_7$  of guanine. Although the two situations may be competitive for some cations,<sup>5c,8</sup> in the case of  $Cu^{2+}$ , adsorption spectra data (chapter 12 of ref 1) seem to indicate that the metal cation is inner sphere bound to nitrogen atoms. Thus, in the present work we have only considered the interaction with  $N_7$ .

Figure 3 presents the optimized structures of  $Cu^{2+}GC$  and  $Ca^{2+}GC$  solvated by five water molecules, as well as the corresponding SPT1 structures. Starting geometries were taken from those previously obtained for  $(H_2O)_5Mg^{2+}GC$ .<sup>10</sup> First, it is observed that in both cases the water molecule interactions change the coordination of the metal cation with guanine. In the gas phase the coordination is bidentate with the  $N_7$  and  $O_6$  of guanine, whereas for the hydrated cations the coordination is monodentate with only  $N_7$ .  $Ca^{2+}$  is hexacoordinated but  $Cu^{2+}$  presents a pentacoordinated structure, with one water molecule in the second solvation shell. This is in agreement with previous studies, which show that  $Ca^{2+}$  has a larger preference to have six water molecules in the first coordination shell.<sup>41</sup> On the other hand, a pentacoordinated structure of  $Cu^{2+}$  has also been reported for  $(H_2O)_5Cu^{2+}PO_4^-$ .<sup>16</sup>

It should be mentioned that for  $(H_2O)_5Cu^{2+}GC$  we have also been able to locate a structure with the five water molecules directly interacting with  $Cu^{2+}$ . However, this structure lies 6.7 kcal/mol higher in energy with basis set B1. Moreover, upon transferring the  $N_1-H$  proton to cytosine in the hexacoordinated complex, one water molecule moved to the second solvation shell. Because of that and for consistency we only report the geometry of the pentacoordinated  $H_2O-(H_2O)_4Cu^{2+}GC$  complex. On the other hand, because previous studies on  $Zn^{2+}-(H_2O)_6$ <sup>40</sup> and  $Cu^+(H_2O)_n$  ( $n = 4, 5$ )<sup>38</sup> have shown that the energy cost for changing the local environment of the metal cation is small, and that  $Cu^{2+}(H_2O)_n$  clusters present a certain preference for a planar tetragonal hydration shell,<sup>42</sup> we have analyzed the  $(H_2O)_4Cu^{2+}GC$  complex in more detail and considered different situations according to the number of water molecules directly bonded to the metal cation. These configurations will be denoted as  $(m,n)$  where  $m$  is the number of molecules interacting with  $Cu^{2+}$  and  $n$  equals the number of water molecules in the second solvation shell.

We have not attempted to explore exhaustively the potential energy surface of these complexes, because it is very complex due to the high number of relative minima associated with the water molecules orientation and also computationally very demanding due to the size of the system. Our main goal has been to analyze the influence of the number of water bonds to the metal cation on the base pairing and on the reaction energy of the single-proton-transfer reaction. For that we have chosen some representative complexes. Particularly interesting is how the different environments modify the oxidant character of  $Cu^{2+}$ .

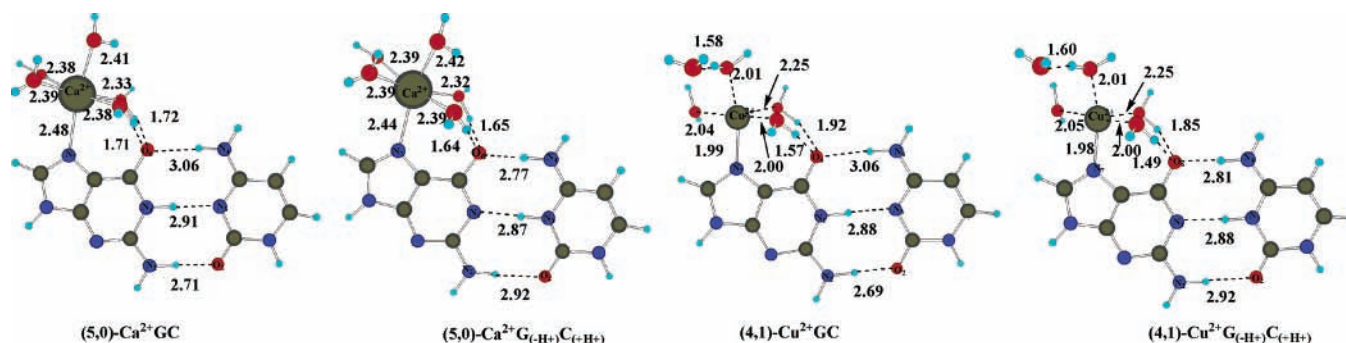


**Figure 3.** B3LYP/B1 optimized geometries for  $(\text{H}_2\text{O})_5\text{M}^{2+}\text{GC}$  and  $(\text{H}_2\text{O})_5\text{M}^{n+} \text{G}^-(\text{H}^+)\text{C}^+(\text{H}^+)$  ( $\text{M} = \text{Ca}^{2+}$  and  $\text{Cu}^{2+}$ ) systems. Distances are in Å.

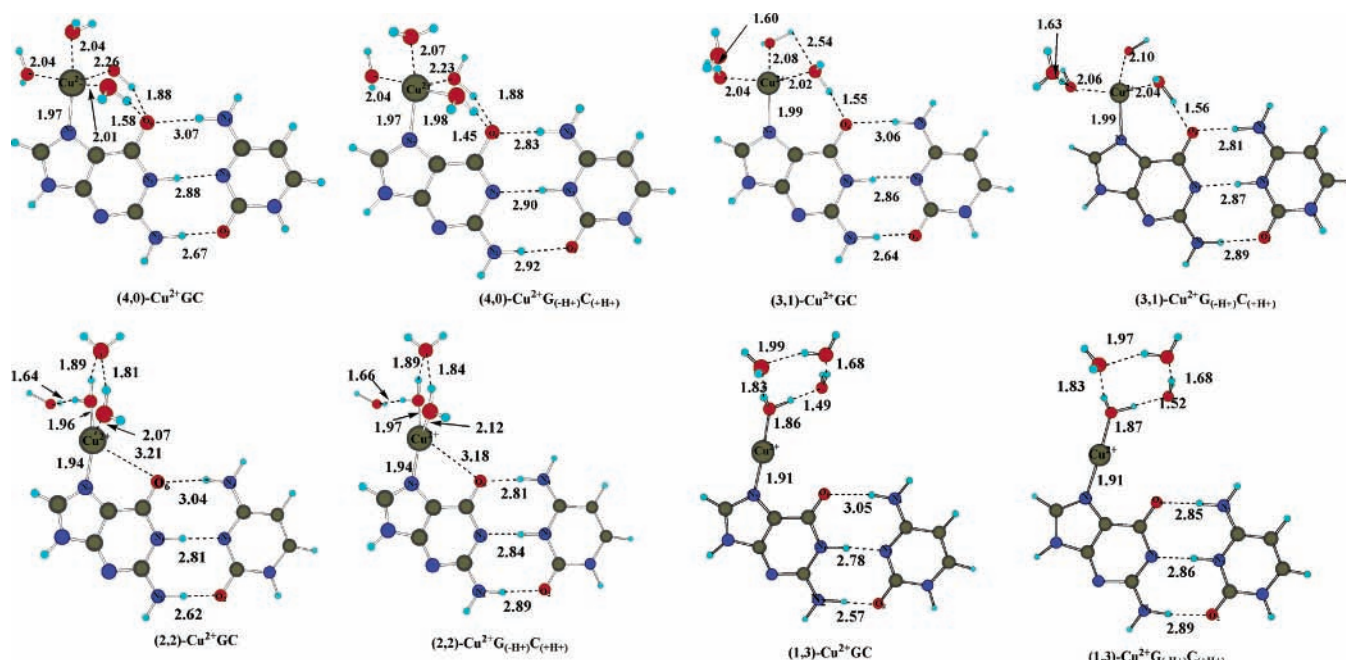


**Figure 4.** B3LYP/B1 optimized geometries for  $(m,n)\text{Cu}^{2+}\text{GC}$  and  $(m,n)\text{Cu}^{2+} \text{G}^-(\text{H}^+)\text{C}^+(\text{H}^+)$  for  $m + n = 4$ . Distances are in Å.

Figure 4 shows the optimized structures for  $(\text{H}_2\text{O})_4\text{Cu}^{2+}\text{GC}$  and the corresponding proton-transferred structures for different  $(m,n)$  coordinations.

The pentacoordinated  $(4,0)\text{Cu}^{2+}\text{GC}$  system shows a square pyramid structure. The  $\text{N}_7$  and the three oxygens more closely interacting with the metal lie more or less in the same plane. The fourth water molecule, with a larger metal–oxygen distance, is more weakly bound and is located at the axial position. The geometry of the tetracoordinated  $(3,1)\text{Cu}^{2+}\text{GC}$  complex is something between tetrahedra and a square planar. The  $(2,2)\text{Cu}^{2+}\text{GC}$  system is three-coordinated with a planar trigonal geometry, whereas that of dicoordinated  $(1,3)\text{Cu}^{2+}\text{GC}$  is linear.

It can be observed in Table 5 that the degree of metal oxidation depends on the coordination environment. For the highly coordinated  $(4,0)\text{Cu}^{2+}\text{GC}$  system, population analysis shows that that copper behaves as  $\text{Cu}^{2+}$  given that the spin density mainly lies at this atom (0.69), as expected for a  $d^9$  open-shell cation. The net atomic charge of  $\text{Cu}^{2+}$  is significantly smaller than 2 because of water to metal electron donation. However, for the less coordinated  $(1,3)$  complex, the spin density mainly lies on guanine (0.97), the charge on this monomer being 0.86. Thus, copper behaves as  $\text{Cu}^+$  and as for the nonhydrated system, the metal induces an oxidation of guanine, the final complex behaving as  $(1,3)\text{Cu}^+\text{G}^+\text{C}$ . For the tricoordinated  $(2,2)$  system, there is still an important charge transfer from guanine to  $\text{Cu}^{2+}$ , the spin density on guanine being 0.75. Finally, the tetracoordinated  $(3,1)\text{Cu}^{2+}\text{GC}$  complex shows an intermediate

**TABLE 5: B3LYP Reaction Energies of the Single-Proton-Transfer Reaction (SPT1) Computed with Basis Sets B1 and B2 (kcal/mol) and Charge and Spin at the Metal and Guanine Monomer from Natural Population Analysis<sup>a</sup>**

$(m,n)\text{M}^{n+}\text{GC}$	$\Delta E$		charge		spin	
	B1	B2	$\text{M}^{2+}$	G	$\text{M}^{2+}$	G
$(0,0)\text{Ca}^{2+}\text{GC}$	-4.3	-3.8	1.85	-0.01		
$(0,0)\text{Cu}^{2+}\text{GC}$	-10.7	-10.1	0.90	0.81	0.00	0.98
$(5,0)\text{Ca}^{2+}\text{GC}$	+2.3		1.77	0.04		
$(4,1)\text{Cu}^{2+}\text{GC}$	-0.6		1.39	0.17	0.70	0.11
$(4,0)\text{Cu}^{2+}\text{GC}$	-0.6	-0.9	1.38	0.19	0.69	0.13
$(3,1)\text{Cu}^{2+}\text{GC}$	-2.2	-2.4	1.20	0.42	0.48	0.42
$(2,2)\text{Cu}^{2+}\text{GC}$	-3.0	-3.0	0.97	0.66	0.21	0.75
$(1,3)\text{Cu}^{2+}\text{GC}$	-5.8	-5.6	0.75	0.86	0.01	0.97

<sup>a</sup>  $m$  indicates the number of water molecules directly coordinated to the metal cation, and  $n$ , the number of water molecules in the second hydration shell.

situation, guanine being only partially oxidized. Thus, the ability of copper cation to oxidize guanine depends on the number of water molecules directly interacting with the metal. Also, the kind of coordination of water molecules can contribute to favor or not the electron transfer, square planar coordinations stabilizing the  $\text{Cu}^{2+}$  oxidation state.

Figure 5 shows the open-shell orbitals of  $(\text{H}_2\text{O})_4\text{Cu}^{2+}\text{GC}$  for the different  $(m,n)$  situations. In agreement with the spin distribution, the open-shell orbital of  $(4,0)\text{Cu}^{2+}\text{GC}$  is mainly

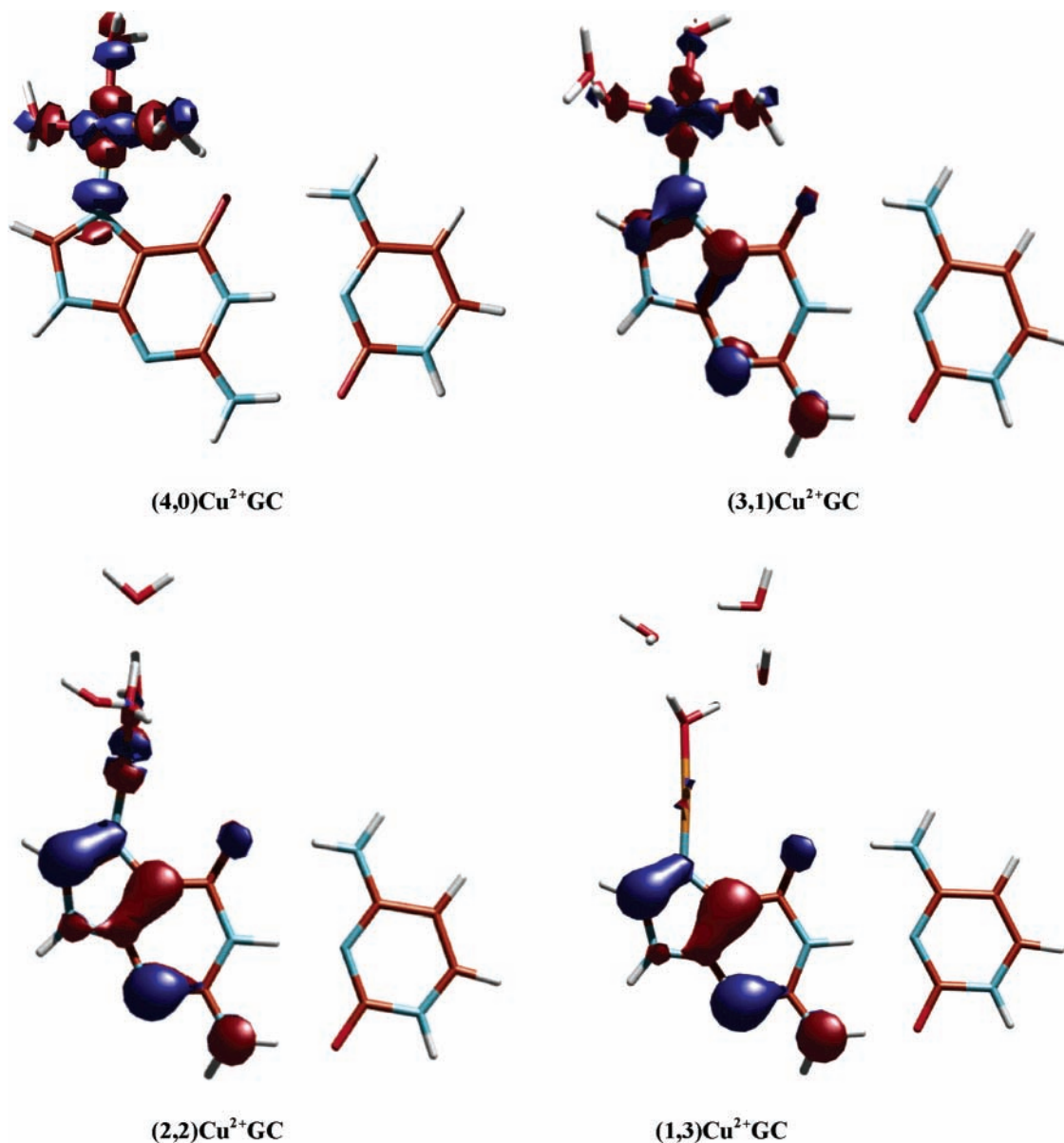


Figure 5. Open-shell orbitals of different  $(m,n)\text{Cu}^{2+}\text{GC}$  complexes.

centered at the metal cation, whereas that of  $(3,1)\text{Cu}^{2+}\text{GC}$  and  $(2,2)\text{Cu}^{2+}\text{GC}$  is more delocalized on the metal and guanine fragments. For  $(1,3)\text{Cu}^{2+}\text{GC}$  this orbital mainly corresponds to the HOMO orbital guanine, the contribution of the 3d orbitals of copper being very small. This different behavior depending on the arrangement of the water molecules around the metal cation can be understood considering the metal–ligand interactions. For  $(4,0)$ , the optimized geometry corresponds to a square pyramid like structure with three water molecules and guanine coordinating the metal cation more or less in the same plane. The ligands in this plane ( $xy$ ) largely destabilize the  $d_{x^2-y^2}$  orbital of the metal cation and so, the preferred situation corresponds to having this orbital monoccupied. However, for  $(3,1)$  with a more tetrahedral like disposition than square planar, or for the trigonal  $(2,2)$  complex the ligand field splitting is smaller; that is, the 3d orbitals are less destabilized, which favors the electron transfer from guanine to the metal cation. For  $(1,3)$  with a linear coordination, the highest  $3d\sigma$  orbital is even less destabilized, because it mixes with the 4s orbital to reduce metal–ligand repulsion.<sup>39</sup> Thus, in this case the preferred situation corresponds to having the singly occupied orbital on guanine.

Previous results have shown that the interaction of naked metal cations with guanine modifies the hydrogen bonds of the guanine–cytosine base pair: the  $\text{O}_6\text{--N}_4$  H-bond distance increases whereas the other two,  $\text{N}_1\text{--N}_3$  and  $\text{N}_2\text{--O}_2$ , decrease, especially the latter one. These changes were especially pronounced for  $\text{Cu}^{2+}$  (see Table 1). The comparison between the H-bond distances obtained for  $(\text{H}_2\text{O})_5\text{--M}^{2+}\text{--GC}$  (see Figure 3) and naked  $\text{M}^{2+}\text{--GC}$  (Table 1) for  $\text{Ca}^{2+}$  and  $\text{Cu}^{2+}$  shows that when the metal cation is hydrated, the changes are not so important due to the screening of the metal charge. On the other hand, the geometries obtained for the  $(4,1)\text{Cu}^{2+}\text{GC}$  and  $(4,0)\text{Cu}^{2+}\text{GC}$  are very similar (see Figures 3 and 4), indicating that the effect of the water molecule on the second solvation shell is not important. However, the hydrogen bond distances of the guanine–cytosine base pair vary significantly according to the number of water molecules directly interacting with  $\text{Cu}^{2+}$ . For example, the  $\text{N}_2\text{--O}_2$  hydrogen bond changes from 2.67 Å for  $(4,0)\text{Cu}^{2+}\text{GC}$  to 2.57 Å for  $(1,3)\text{Cu}^{2+}\text{GC}$ . For the nonhydrated  $\text{Cu}^{2+}\text{GC}$  system this value is 2.51 Å. Therefore, the larger the number of water molecules bonded to the metal cation the smaller the effect of metal cationization on the guanine–cytosine

**TABLE 6: Relative Energies (kcal/mol) of  $(\text{H}_2\text{O})_{m+n}\text{Cu}^{2+}\text{GC}$  and  $(\text{H}_2\text{O})_{m+n}\text{Cu}^{2+}\text{G}^-_{(-\text{H}^+)}\text{C}^+_{(+\text{H}^+)}$  Systems<sup>a</sup> Computed at the B3LYP Level with Basis Sets B1 and B2**

$(m,n)$	$(\text{H}_2\text{O})_{m+n}\text{Cu}^{2+}\text{GC}$		$(\text{H}_2\text{O})_{m+n}\text{Cu}^{2+}\text{G}^-_{(-\text{H}^+)}\text{C}^+_{(+\text{H}^+)}$	
	B1	B2	B1	B2
(4,0)Cu <sup>2+</sup> GC	0.8	5.7	3.2	7.9
(3,1)Cu <sup>2+</sup> GC	0.3	2.4	1.0	3.0
(2,2)Cu <sup>2+</sup> GC	0.0	0.0	0.0	0.0
(1,3)Cu <sup>2+</sup> GC	4.5	3.4	1.6	0.8

<sup>a</sup>  $m$  indicates the number of water molecules directly coordinated to the metal cation, and  $n$ , the number of water molecules in the second hydration shell.

base pair. Although this was to be expected due to the screening of electrostatic effects, it is remarkable that even for the highly coordinated (4,0) or (3,1) environments the induced changes are similar to or larger than those found for the unsolvated  $\text{Ca}^{2+}$ -GC system. This is due in part to the fact that  $\text{Cu}^{2+}$  shows a smaller metal-guanine distance than  $\text{Ca}^{2+}$  but also to the oxidant character of  $\text{Cu}^{2+}$ , which partly remains in the hydrated complexes.

Population analysis of the proton-transferred structures, SPT1, show that the spin distribution in the different environments is preserved along the reaction. With respect to the hydrogen bonds, the most important change observed upon hydration of the metal cation is that the  $\text{O}_6$ - $\text{N}_4$  hydrogen bond in which cytosine acts as a proton donor becomes significantly shorter than in the nonhydrated system, due to the screening of the repulsive electrostatic interaction.

The proton-transfer reaction energies with basis sets B1 and B2 are shown in Table 5. The computed reaction energies with the two basis sets are quite similar, the largest differences being 0.6 kcal/mol for naked  $\text{Cu}^{2+}\text{GC}$ . As expected, the proton-transfer reaction is disfavored by the hydration of the metal cation. For  $\text{Ca}^{2+}$ , the reaction energy with basis set B1 changes from  $-4.3$  to  $+2.3$  kcal/mol. For  $\text{Cu}^{2+}$ , hydration of the metal also disfavors the reaction from  $-10.7$  to  $-0.6$  kcal/mol for the highly coordinated (4,1) and (4,0) complexes. For the other (3,1), (2,2), and (1,3) complexes the reaction energy varies depending on the coordination environments. The smaller the number of water molecules directly interacting with  $\text{Cu}^{2+}$ , the more negative becomes the reaction energy. The obtained values range from  $-0.6$  kcal/mol for (4,0) to  $-5.8$  kcal/mol for (1,3). Such variations are due both to the changes on the electrostatic and oxidant effects. However, one observed trend is that the larger is the degree of oxidation of guanine, the most favorable becomes the proton-transfer reaction, which points out the importance of oxidative effects of  $\text{Cu}^{2+}$ .

One interesting point to look at is which of the  $(m,n)\text{Cu}^{2+}$ -GC clusters is the most stable one. The relative energies of the different  $(m,n)$  complexes for the nontransferred  $(\text{H}_2\text{O})_4\text{Cu}^{2+}$ -GC and the single-proton-transferred  $(\text{H}_2\text{O})_4\text{Cu}^{2+}\text{G}^-_{(-\text{H}^+)}\text{C}^+_{(+\text{H}^+)}$  systems are given in Table 6. Both for the nontransferred and the single-proton-transferred species, and with the two basis sets the three coordinated (2,2) complexes are the most stable ones. However, the relative energies change significantly when enlarging the basis set.

The relative energy of the different coordination environments arises from many factors. On one hand, when one water molecule moves from the first to the second solvation shell, one metal-water interaction is lost but new hydrogen bond interactions between water molecules appear. These hydrogen bond interactions are stronger than that of two isolated waters because the water molecules interacting with the metal cation are more acidic due to water polarization and charge transfer.

Moreover, metal-ligand and ligand-ligand repulsion decrease when decreasing the number of water molecules directly interacting with the metal cation. On the other hand, as seen previously, the local environment of the metal cation determines the oxidizing power of  $\text{Cu}^{2+}$ , in such a way that the small coordination number favors the oxidation of guanine and consequently the guanine-cytosine base pair interaction is strengthened. Thus, the relative energies result from a subtle balance of many different factors.

The small relative energies between the different coordination arrangements agree with previous studies<sup>8,38,40,43</sup> that show the flexibility of the cation hydration shell. It must be mentioned, however, that the relative energies between different structures may be quite sensitive to the level of theory used or basis set, especially in the present case where different coordination environments lead to different oxidation states of the metal cation. Calculations using larger basis sets or post Hartree-Fock methods, however, cannot be performed for the present systems because they are computationally too demanding. Therefore, although the larger basis set used in the present study is reasonable, the obtained relative energies are too small to draw definitive conclusions about which is the preferred coordination. What appears to be clear is that the coordination sphere of  $\text{Cu}^{2+}$  is very flexible and that certain local environments of the metal can induce the oxidation of guanine and, as a consequence, favor the mutagenic<sup>15</sup> proton-transfer reaction to cytosine. Although the studied clusters are simplified models that do not take into account all the complexity of a living system, we expect that the present results can provide new insights on the effects of  $\text{Cu}^{2+}$  binding to DNA bases, which are different from other divalent cations.

#### IV. Conclusions

This work analyzes the influence of metal cations coordinated to  $\text{N}_7$  of guanine on the intermolecular proton-transfer reaction in guanine-cytosine base pairs. Gas phase calculations on  $\text{M}^{n+}$ -GC ( $\text{M} = \text{Cu}^+$ ,  $\text{Ca}^{2+}$ , and  $\text{Cu}^{2+}$ ) show that the interaction of the metal cation stabilizes the ion pair structure derived from the  $\text{N}_1$ - $\text{N}_3$  single-proton-transfer reaction, the effects being more pronounced for the divalent cations than for the monovalent one. Therefore, the process turns from thermodynamically unfeasible to thermodynamically favorable when both  $\text{Ca}^{2+}$  and  $\text{Cu}^{2+}$  interact with  $\text{N}_7$  of guanine. For  $\text{Cu}^{2+}\text{GC}$  the proton transfer is largely favored ( $\Delta E = -10.1$  kcal/mol) due to both electrostatic and oxidative effects.

The effect of a reduced number of solvating water molecules has also been considered for the divalent  $\text{Ca}^{2+}$  and  $\text{Cu}^{2+}$ . As expected, the presence of water molecules disfavors the reaction due to the screening of electrostatic effects. However, for  $\text{Cu}^{2+}$  the reaction can still be easily produced, especially for certain local environment of the metal cation. Results show that the oxidant power of the  $\text{Cu}^{2+}$  depends on the number of water molecules directly interacting with the metal cation and on their geometrical disposition. Pentacoordinated complexes with a square pyramid geometry stabilize the  $\text{Cu}^{2+}$  oxidation state whereas for the tetra- or tricoordinated complexes an important charge transfer from guanine to  $\text{Cu}^{2+}$  takes place. It is found that there is a direct relation between the degree of oxidation of guanine and the reaction energy of the studied process, the larger the oxidation degree of guanine, the more favorable the proton-transfer reaction. Therefore, the ability of  $\text{Cu}^{2+}$  to oxidize guanine turns out to be a key factor for this mutagenic process. Moreover, the fact that  $\text{Cu}^{2+}$  cations are closely associated with DNA bases might explain why this cation has been found to induce DNA damage through base pair modification.



**Acknowledgment.** Financial support from MCYT and FEDER (project BQU2002-04112-C02-01), DURSI (project 2001SGR-00182) and the use of the computational facilities of the Catalonia Supercomputer Center (CESCA) and the Center of Parallelism of Barcelona (CEPBA) are gratefully acknowledged. M.S. is indebted to the Departament d'Universitats, Recerca i Societat de la Informació (DURSI) of the Generalitat de Catalunya for financial support.

## References and Notes

- (1) *Metal ions in biological systems: Interactions of metal ions with nucleotides, nucleic acids, and their constituents*; Sigel, A. Sigel, H., Eds.; Marcel Dekker: New York, 1996; Vol. 32.
- (2) Lippert, B. *Coord. Chem. Rev.* **2000**, *200*, 487–516.
- (3) Martin, R. B.; *Acc. Chem. Res.* **1985**, *18*, 32–38.
- (4) Burda, J. V.; Šponer, J.; Hobza, P. *J. Phys. Chem.* **1996**, *100*, 7250–7255.
- (5) (a) Cerda, B. A.; Wesdemiotis, C. *J. Am. Chem. Soc.* **1996**, *118*, 11884–11892. (b) Russo, N.; Toscano, M.; Grand, A. *J. Am. Chem. Soc.* **2001**, *123*, 10272–10279. (c) Petrov, A. S.; Lamm, G.; Pack, G. R. *J. Phys. Chem. B* **2002**, *106*, 3294–3300.
- (6) (a) Fonseca Guerra, C.; Bickelhaupt, F. M.; Snijders, J. G.; Baerends, E. J. *J. Am. Chem. Soc.* **2000**, *122*, 4117–4128. (b) Fonseca Guerra, C.; Bickelhaupt, F. M. *Angew. Chem., Int. Ed. Engl.* **1999**, *38*, 2942–2945.
- (7) Gadre, S. R.; Pundlik, S. S.; Limaye, A. C.; Rendell, A. P. *Chem. Commun.* **1998**, 573–574.
- (8) Gresh, N.; Šponer, J. *J. Phys. Chem. B* **1999**, *103*, 11415–11427.
- (9) Šponer, J.; Sabat, M.; Gorb, L.; Leszczynski, J.; Lippert, B.; Hobza, P. *J. Phys. Chem. B* **2000**, *104*, 7535–7544.
- (10) Muñoz, J.; Šponer, J.; Hobza, P.; Orozco, M.; Luque, F. J. *J. Phys. Chem. B* **2001**, *105*, 6051–6060.
- (11) (a) Burda, J. V.; Šponer, J.; Leszczynski, J.; Hobza, P. *J. Phys. Chem. B* **1997**, *101*, 9670–9677. (b) Šponer, J.; Burda, J. V.; Sabat, M.; Leszczynski, J.; Hobza, P. *J. Phys. Chem. A* **1998**, *102*, 5951–5957.
- (12) Burda, J. V.; Šponer, J.; Leszczynski, J. *J. Phys. Chem. Chem. Phys.* **2001**, *3*, 4404–4411.
- (13) Sigel, R. K. O.; Lippert, B. *Chem. Commun.* **1999**, 2167–2168.
- (14) Pelmenschikov, A.; Zilberberg, I.; Leszczynski, J.; Famulari, A.; Sironi, M.; Raimondi, M. *Chem. Phys. Lett.* **1999**, *314*, 496–500.
- (15) Löwdin, P.-O. *Rev. Modern. Phys.* **1963**, *35*, 724–732.
- (16) Rulíšek, L.; Šponer, J. *J. Phys. Chem. B* **2003**, *107*, 1913–1923.
- (17) Gao, Y. G.; Sriram, M.; Wang, A. H. *J. Nucl. Acid Res.* **1993**, *21*, 4093–4191.
- (18) Liang, Q.; Dedon, P. C. *Chem. Res. Toxicol.* **2001**, *14*, 416–422.
- (19) Bal, W.; Kasprzak, K. S. *Toxicol. Lett.* **2002**, *127*, 55–62.
- (20) Lee, D.-H.; O'Connor, T. R.; Pfeifer, G. P. *Nucl. Acids Res.* **2002**, *30*, 3566–3573.
- (21) Drouin, R.; Rodríguez, H.; Gao, S.-W.; Gebreyes, Z.; O'Connor, T. R.; Holmquist, G. P.; Akman, S. A. *Free Radiat. Biol. Med.* **1996**, *21*, 261–273.
- (22) Burrows, C. J.; Muller, J. G. *Chem. Rev.* **1998**, *98*, 1109–1151.
- (23) (a) Bertran, J.; Oliva, A.; Rodríguez-Santiago, L.; Sodupe, M. *J. Am. Chem. Soc.* **1998**, *120*, 8159–8167. (b) Li, X.; Cai, Z.; Sevilla, M. D. *J. Phys. Chem. B* **2001**, *105*, 10115–10123. (c) Li, X.; Cai, Z.; Sevilla, M. D. *J. Phys. Chem. A* **2002**, *106*, 9345–9251.
- (24) (a) Becke, A. D. *J. Chem. Phys.* **1993**, *98*, 5648–5652. (b) Lee, C.; Yang, W.; Parr, R. G. *Phys. Rev. B* **1988**, *37*, 785–789. (c) Stephens, P. J.; Devlin, F. J.; Chabalowski, C. F.; Frisch, M. J. *J. Phys. Chem.* **1994**, *98*, 11623–11627.
- (25) Frisch, M. J.; Trucks, G. W.; Schlegel, H. B.; Scuseria, G. E.; Robb, M. A.; Cheeseman, J. R.; Zakrzewski, V. G.; Montgomery, J. A., Jr.; Stratmann, R. E.; Burant, J. C.; Dapprich, S.; Millam, J. M.; Daniels, A. D.; Kudin, K. N.; Strain, M. C.; Farkas, O.; Tomasi, J.; Barone, V.; Cossi, M.; Cammi, R.; Mennucci, B.; Pomelli, C.; Adamo, C.; Clifford, S.; Ochterski, J.; Petersson, G. A.; Ayala, P. Y.; Cui, Q.; Morokuma, K.; Malick, D. K.; Rabuck, A. D.; Raghavachari, K.; Foresman, J. B.; Cioslowski, J.; Ortiz, J. V.; Baboul, A. G.; Stefanov, B. B.; Liu, G.; Liashenko, A.; Piskorz, P.; Komaromi, I.; Gomperts, R.; Martin, R. L.; Fox, D. J.; Keith, T.; Al-Laham, M. A.; Peng, C. Y.; Nanayakkara, A.; Gonzalez, C.; Challacombe, M.; Gill, P. M. W.; Johnson, B.; Chen, W.; Wong, M. W.; Andres, J. L.; Gonzalez, C.; Head-Gordon, M.; Replogle, E. S.; Pople, J. A. *Gaussian 98*; Gaussian, Inc.: Pittsburgh, PA, 1998.
- (26) See, for example: (a) Ricca, A.; Bauschlicher, C. W. *Chem. Phys. Lett.* **1995**, *245*, 150–157. (b) Blomberg, M. R. A.; Siegbahn, P. E.; Svensson, M. *J. Chem. Phys.* **1996**, *104*, 9546–9554. (c) Barone, V.; Adamo, C.; Mele, F. *Chem. Phys. Lett.* **1996**, *249*, 290–296. (d) Holthausen, M. C.; Mohr, M.; Koch, W. *Chem. Phys. Lett.* **1995**, *240*, 245–252. (e) Sodupe, M.; Branchadell, V.; Rosi, M.; Bauschlicher, C. W. *J. Phys. Chem. A* **1997**, *101*, 7854–7859. (f) Luna, A.; Alcamí, M.; Mo, O.; Yañez, M. *Chem. Phys. Lett.* **2000**, *320*, 129–138. (g) Bauschlicher, C. W.; Ricca, A.; Partridge, H.; Langhoff, S. R. In *Recent Advances in Density Functional Theory, Part II*; Chong, D. P., Ed.; World Scientific Publishing Co.: Singapore, 1997.
- (27) Wachters, A. J. H. *J. Chem. Phys.* **1970**, *52*, 1033–1036.
- (28) Hay, P. J. *J. Chem. Phys.* **1977**, *66*, 4377–4384.
- (29) Raghavachari, K.; Trucks, G. W. *J. Chem. Phys.* **1989**, *91*, 1062–1065.
- (30) Blaudeau, J.-P.; McGrath, M. P.; Curtiss, L. A.; Radom, L. *J. Chem. Phys.* **1997**, *107*, 5016–5021.
- (31) Boys, B. S.; Bernardi, F. *Mol. Phys.* **1970**, *19*, 553.
- (32) McQuarrie, D. *Statistical Mechanics*; Harper and Row: New York, 1986.
- (33) (a) Weinhold, F.; Carpenter, J. E. *The structure of small molecules and ions*; Plenum: New York, 1988. (b) Reed, A. E.; Curtiss, L. A.; Weinhold, F. *Chem. Rev.* **1988**, *88*, 899–926.
- (34) Song, B.; Zhao, J.; Griesser, R.; Meiser, C.; Sigel, H.; Lippert, B. *Chem. Eur. J.* **1999**, *5*, 2374–2387.
- (35) Russo, N.; Toscano, M.; Grand, A.; Jolibois, F. *J. Comput. Chem.* **1998**, *19*, 989–1000.
- (36) Florián, J.; Leszczyński, J. *J. Am. Chem. Soc.* **1996**, *118*, 3010–3017.
- (37) Bock, C. W.; Kaufman, A.; Glusker, J. P. *Inorg. Chem.* **1994**, *33*, 419–427.
- (38) Feller, D.; Glendening, E. D.; de Jong, W. A. *J. Chem. Phys.* **1999**, *110*, 1475–1491.
- (39) Bauschlicher, C. W.; Langhoff, S. R.; Partridge, H. *J. Chem. Phys.* **1991**, *94*, 2068–2072.
- (40) Bock, C. W.; Katz, A. K.; Glusker, J. P. *J. Am. Chem. Soc.* **1995**, *117*, 3754–3765.
- (41) Katz, A. K.; Glusker, J. P.; Beebe, S. A.; Bock, C. W. *J. Am. Chem. Soc.* **1996**, *118*, 5752–5763.
- (42) Bérces, A.; Nukada, T.; Margl, P.; Ziegler, T. *J. Phys. Chem. A* **1999**, *103*, 9693–9701.
- (43) Šponer, J.; Burda, J. V.; Leszczynski, J.; Hobza, P. *J. Biomol. Struct. Dynam.* **1999**, *17*, 61–77.